Heat Mass Transfer (2009) 45:1247–1251
DOI 10.1007/s00231-009-0493-x

ORIGINAL

Cut-off cooling velocity profiling inside a keyhole model using the Boubaker polynomials expansion scheme

S. Amir Hossein A. E. Tabatabaei · Tinggang Zhao · O. Bamidele Awojoyogbe · Folorunsho O. Moses

Received: 27 October 2008 / Accepted: 24 April 2009 / Published online: 6 June 2009

Abstract The time dependent heating and cooling velocities are investigated in this paper. The temperature profile is found by using a keyhole approximation for the melted zone and solving the heat transfer equation. A polynomial expansion has been deployed to determine the cooling velocity during welding cut-off stage. The maximum cooling velocity has been estimated to be $V_{max} \approx 83°C\ s^{-1}$.

List of symbols

- D Thermal diffusivity ($m^2\ s^{-1}$)
- h Keyhole height (m)
- k Thermal conductivity ($Wm^{-1}\ K^{-1}$)
- N_0 Prefixed integer
- P Fluid pressure at mean temperature (Pa)
- Q_v Power per unit volume (Wm^{-3})
- T Absolute temperature (K)
- T_0 Maximum absolute temperature (K)
- T_∞ Room absolute temperature (K)

S. A. H. A. E. Tabatabaei (✉)
Sadra Institute of Higher Education, Tehran, Iran
e-mail: tabatabaei.amirhossein@gmail.com

T. Zhao
College of Mathematics, Lanzhou City University,
Lanzhou, Gansu, People's Republic of China
e-mail: chz.khl2008@ymail.com

O. B. Awojoyogbe
Department of Physics, Federal University of Technology,
Minna, Niger State, Nigeria

F. O. Moses
Department of Physics, Federal University of Technology,
Akure, Ondo State, Nigeria

Greek letters

- α_q Boubaker polynomials minimal positive roots (dimensionless)
- ϖ Constant (dimensionless)
- ρ Density (Kg m^{-3})
- γ Heat capacity ratio (dimensionless)
- ξ_q Real coefficients (dimensionless)

1 Introduction

The demand for high power lasers for precise welding has been increased in the last decades. Simultaneous to this trend, laser welding computation techniques have been improved to the point where numerical modelling [1–6] began more and more acceptable as a guide to the prediction of geometries of weld and the profile of temperature.

The laser welding keyhole (Fig. 1) model was proposed in the earliest studies as an alternative to both Gaussian and Double Ellipsoidal (DE) models. In the end of the last decade, two relevant models were consecutively proposed and discussed by Singh et al. [1] and Anisimov [2]. The latter model was more realistic, since it did not adopt the assumption of isothermal expansion inside the keyhole.

In this study, we tried to set a cylindrical model as a guide to solve the heat equation inside the heated keyhole and evaluate the cooling velocity in the relaxation phase.

2 Keyhole model features

For establishing the keyhole approximation model, we presumed that the keyhole vertical edges temperature is

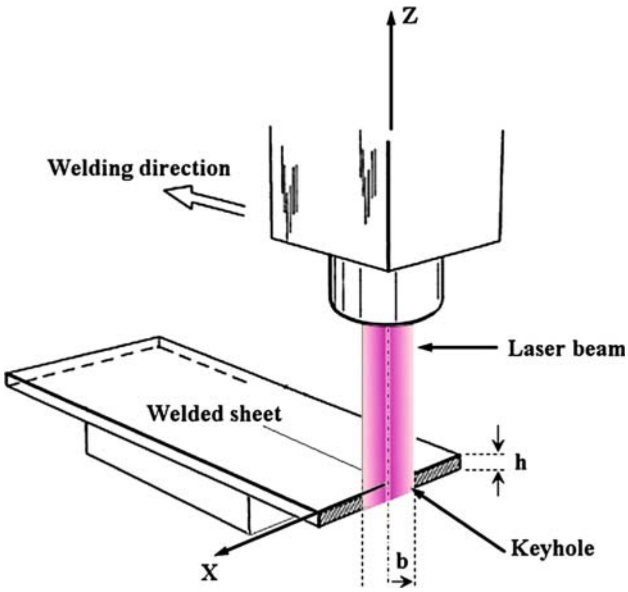

Fig. 1 Laser welding disposal

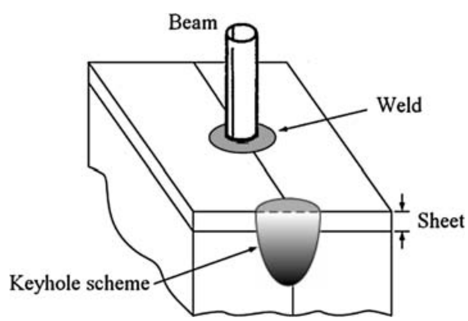

Fig. 2 Keyhole scheme

equal to the boiling point of the material and that the heat transfer along directions perpendicular to the incident laser beam is invariant under cylindrical symmetry.

Parallel to these assumptions, it as supposed that the heat source is Gaussian (Fig. 2) and centred along the keyhole axis. The exciting beam thermal and optical profiles were also supposed to be coherent.

The source cut-off date was set as the starting point of the modelling procedure.

It was also supposed that keyhole dimensions h and b (Fig. 1), are small when compared to bulk.

3 Theory

First, the maximal central temperature T_0 is obtained analogically to Coulomb approximation [7, 8]:

$$T_0 = \frac{\hat{P}}{2\pi k}\frac{1}{\hat{b}} \tag{1}$$

where k is the thermal conductivity, $\hat{P}$ and $\hat{b}$ are defined by:

$$\begin{cases} \hat{b} = \dfrac{2b}{\sqrt{\pi}} \\ \hat{P} = \displaystyle\int_{-h}^{0}\left(\int_{0}^{+\infty} Q_v \times \mathrm{e}^{-\frac{x^2}{2b^2}} 2\pi x \mathrm{d}x\right)\mathrm{d}z = \dfrac{8P_{ak}}{\sqrt{\pi}} \end{cases} \tag{2}$$

where Q_v is the power per unit volume absorbed by the keyhole and P_{ak} is the total power absorbed by the keyhole volume:

$$Q_v = \frac{P_{ak}}{V_{\text{keyhole}}} = \frac{4P_{ak}}{h\pi b^2} \tag{3}$$

Maximal central temperature T_0 is then:

$$T_0 = \frac{2P_{ak}}{\pi k b} = \frac{hbQ_v}{2k} \tag{4}$$

The main heat equation inside the keyhole is then:

$$\begin{cases} \dfrac{\partial T(x,t)}{\partial \mathrm{t}} = \dfrac{1}{D}\dfrac{\partial^2 T(x,t)}{\partial \mathrm{x}^2}, t > 0; |x| < b \\ T(x,t)|_{t=0} = \dfrac{hbQ_v}{2k} \times \mathrm{e}^{-\frac{x^2}{2b^2}}; T(x,t)|_{t\to\infty} = T_\infty \end{cases} \tag{5}$$

where T_∞ is the room temperature and D is the thermal diffusivity.

$T(x, t)$ is first expressed as an infinite sum of the Boubaker polynomials [9–13], whose expression fits boundary condition.

$$T(x,t) = T_0 \times \mathrm{e}^{-\frac{x^2}{2b^2}} \times \frac{1}{2N_0}\sum_{n=1}^{N_0} \xi_n B_{4n}\left(t\frac{\alpha_n}{t_m}\right) \tag{6}$$

where α_n are the minimal positive roots (Fig. 3) of the Boubaker $4n$-order polynomials B_{4n} [9–11], t_{m} is the maximum time range (when the temperature is supposed to be room one), N_0 is an even given integer, T_0 is the calculated maximal central temperature and ξ_n are coefficients which verify the system (7):

$$\begin{cases} \displaystyle\sum_{n=1}^{N_0} \xi_n = -N_0 \\ \displaystyle\sum_{n=1}^{N_0} \xi_n \frac{\alpha_n}{t_m} B'_{4n}(\alpha_n) = 0 \end{cases} \tag{7}$$

The system (7), due to the Boubaker polynomials properties, is reduced to:

$$\begin{cases} \displaystyle\sum_{n=1}^{N_0} \xi_n = -N_0 \\ \displaystyle\sum_{n=1}^{N_0} \xi_n \times u_n = 0; \text{ with}: u_n = \left[\alpha_n^2(\alpha_n^2-1)^2(3\alpha_n^2+4)\right] \end{cases} \tag{8}$$

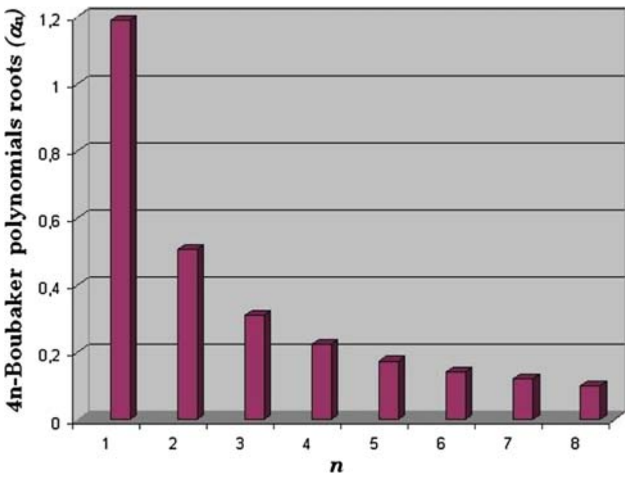

Fig. 3 Minimal positive roots (α_n) of the Boubaker $4n$-order polynomials B_{4n}

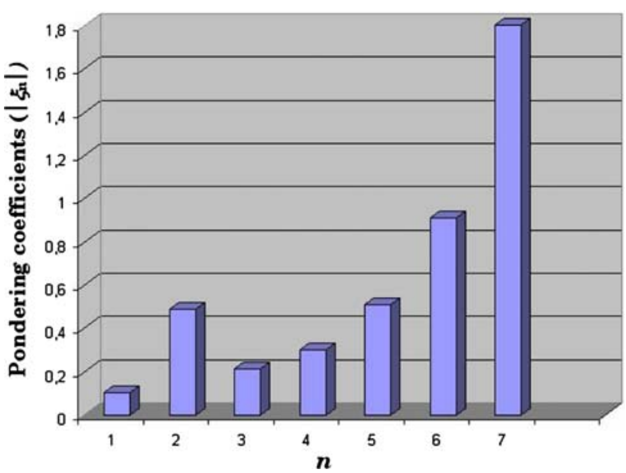

Fig. 4 Absolute value of the coefficients ξ_n

A solution to the system (8) is:

$$\xi_n = \begin{cases} -N_0 \dfrac{u_{(N_0-n+1)}}{\varpi} & \text{if } n < \dfrac{N_0}{2} \\ N_0 \dfrac{u_{(N_0-n+1)}}{\varpi} & \text{if } n > \dfrac{N_0}{2} \\ \text{where } \varpi = \left(\displaystyle\sum_{n=1}^{N_0} u_{(N_0-n+1)} \right) \end{cases} \tag{9}$$

The correspondent calculated parameters are shown in Fig. 4.

4 Results and discussion

The obtained temperature values are presented in Table 1 along with theoretical results.

It is known that a good knowledge of the cooling velocity profile is necessary for predicting and monitoring many interesting items like initial solidification uniformity, slab solidification structure, and metal purity. In this context, the cooling velocity profile (Fig. 5) was derived from the results shown in Table 1. It is noted that the time ($t = 0$) corresponds to the cooling phase starting date ($\approx$0.6 s in Fig. 5).

Table 1 Temperature values versus time

Time (s)	Temperature (measured) (°C)	Temperature (theory) (°C)
0.00	330	–
0.25	421	–
0.50	633	–
0.75	625	–
1.00	621	625
1.25	617	606
1.50	581	584
1.75	574	564
2.00	550	541
2.25	546	544
2.50	540	535
2.75	501	498
3.00	490	468
3.25	485	477
3.50	470	482
3.75	465	466
4.00	452	452
4.25	449	442
4.50	435	430
4.75	422	421
5.00	402	395

Measurement accuracy $\approx$7.5%

The shape of this profile (Fig. 3) is in concordance with the profiles presented by Paul et al. [14], Andreassen et al. [15] and Belcher [16]. The velocity range (0–82°C s^{-1}) is also agreeing with the values published by Santos et al. [17] and more recently by Mughal et al. [18].

5 Conclusion

In this paper, a theoretical–experimental model of heat transfer inside a cylindrical keyhole laser welding [19–28] was presented. We have being tried to exploit the model, by implementing real-time velocity measurements, to prove that the cooling velocity can be reduced by the presence of appropriate alloying elements. This feature is very interesting since it is an issue for hardening with mild quenching. Our numerical results have been compared with both experimental results and recently published results [14–43]. This comparison shows that our model was

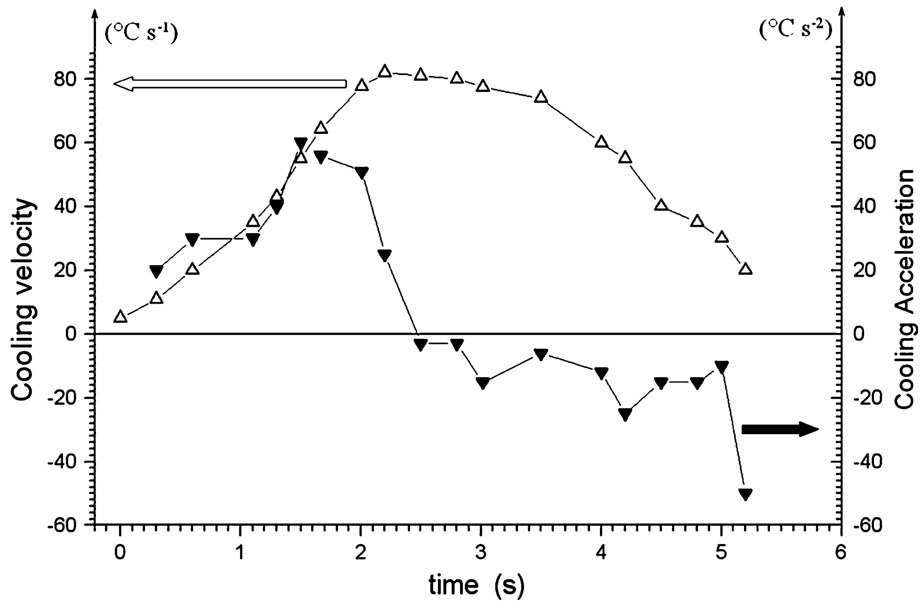

Fig. 5 The cooling velocity and acceleration profiles

well-adapted in order to evaluate the cooling velocity and acceleration.

Acknowledgment The authors would like to acknowledge help and assistance from Associate Professor Karem Boubaker from University of Tunisia.

References

1. Singh RK, Narayan J (1990) Pulsed-laser evaporation technique for deposition of thin films: physics and theoretical model. Phys Rev B 41:8843–8859
2. Anisimov SI, Luk'yanchuk BS, Luches A (1996) An analytical model for three-dimensional laser plume expansion into vacuum in hydrodynamic regime. Appl Surf Sci 96–98:24–32
3. Koopman DW (1971) Langmuir probe and microwave measurements of streaming plasmas generated by focused laser pulses. Phys Fluids 14:1707–1716
4. Toftmann B, Schou J, Hansen TN, Lunney JG (2000) Angular distribution of electron temperature and density in a laser-ablation plume. Phys Rev Lett 84:3998–4001
5. Weaver I, Martin GW, Graham WG, Morrow T, Lewis CLS (1999) The langmuir probe as a diagnostic of the electron component within low temperature laser ablated plasma plumes. Rev Sci Instrum 70:1801–1805
6. Doggett B, Budtz-Joergensen C, Lunney JG, Sheerin P, Turner MM (2005) Behaviour of a planar langmuir probe in a laser ablation plasma. Appl Surf Sci 247:134–138
7. Chaouachi A, Boubaker K, Amlouk M, Bouzouita H (2007) Enhancement of pyrolysis spray disposal performance using thermal time-response to precursor uniform deposition. Eur Phys J Appl Phys 37:105–109
8. Ghanouchi J, Labiadh H, Boubaker K (2008) An attempt to solve the heat transfer equation in a model of pyrolysis spray using 4q-order Boubaker polynomials. Int J Heat Tech 26:49–52
9. Awojoyogbe OB, Boubaker K (2009) A solution to Bloch NMR flow equations for the analysis of homodynamic functions of blood flow system using m-Boubaker polynomials. Curr Appl Phys 9:278–283
10. Boubaker K (2007) On modified Boubaker polynomials: some differential and analytical properties of the new polynomials issued from an attempt for solving bi-varied heat equation. Trends Appl Sci Res 2:540–544 (by Academic Journals 'aj' New York)
11. Labiadh H (2007) A Sturm-Liouville shaped characteristic differential equation as a guide to establish a quasi-polynomial expression to the Boubaker polynomials. J Differ Equ Control Processes 2:117–133
12. Gallusser R, Dressler K (1971) Application of the coulomb approximation to the Rydberg transitions of the NO molecule. Zeitschrift für Angewandte Mathematik und Physik (ZAMP) 22:792–794
13. Armstrong BH, Purdum KL (1966) Extended use of the coulomb approximation: mean powers, a sum rule, and improved transition integrals. Phys Rev 150:51–58
14. Paul A, Debroy T (1988) Free surface flow and heat transfer in conduction mode laser welding. Metall Mater Trans B 19:851–858
15. Andreassen E, Myhre OJ, Oldervoll F, Hinrichsen EL, Grøstad K, Braathen MD (1995) Nonuniform cooling in multifilament melt spinning of polypropylene fibers: cooling air speed limits and fiber-to-fiber variations. J Appl Polym Sci 58:1619–1632
16. Belcher SL (2007) Practical guide to injection blow molding, ISBN 0824757912, 9780824757915, CRC Press, Boca Raton
17. Santos CAC, Quaresma JNN, Lima JA (2001) Convective heat transfer in ducts: the integral transform approach: the integral transform approach, ISBN 8587922238, 9788587922236, E-papers Servicos Editoriais Ltda
18. Mughal MP, Fawad H, Mufti R (2006) Finite element prediction of thermal stresses and deformations in layered manufacturing of metallic parts. Acta Mech 183:61–79
19. Dowden J, Postacioglu N, Davis M, Kapadia P (1987) A keyhole model in penetration welding with a laser. J Phys D Appl Phys 20:36–44
20. Semak VV, Bragg WD, Damkroger B, Kempka S (1999) Transient model for the keyhole during laser welding. J Phys D Appl Phys 32:61–64
21. Ki H, Mazumder J, Mohanty PS (2002) Modeling of laser keyhole welding: Part II. simulation of keyhole evolution, velocity, temperature profile, and experimental verification. Metall Mater Trans A 33:1831–1842

22. Rai R, Kelly SM, Martukanitz RP, DebRoy T (2008) A convective heat-transfer model for partial and full penetration keyhole mode laser welding of a structural steel. Metall Mater Trans A 39:98–112
23. Al-Kazzaz H, Medraj M, Caoand X, Jahazi M (2008) Nd:YAG laser welding of aerospace grade ZE41A magnesium alloy: modeling and experimental investigations. Mater Chem Phys 109:61–76
24. Kaplan A (1994) A model of deep penetration laser welding based on calculation of the keyhole profile. J Phys D Appl Phys 27(180):5–1814
25. Lampa C, Kaplan AFH, Powell J, Magnusson C (1997) An analytical thermodynamic model of laser welding. J Phys D Appl Phys 30(9):1293–1299
26. Jin X, Li L, Zhang Y (2002) A study on Fresnel absorption and reflections in the keyhole in deep penetration laser welding. J Phys D Appl Phys 35:2304–2310
27. Solana GNegro (1997) A study of the effect of multiple reflections on the shape of the keyhole of the keyhole in the laser processing of materials. J Phys D Appl Phys 30:3216–3222
28. Wu CS, Wang HG, Zhang YM (2006) A new heat source model for keyhole plasma arc welding in FEM analysis of the temperature profile. Weld J 85:284–289
29. Yamamoto N, Genma K (2007) On error estimation of finite element approximations to the elliptic equations in nonconvex polygon domains. J Comput Appl Math 199:286–296
30. Tabata M (2007) Discrepancy between theory and real computation on the stability of some finite element schemes. J Comput Appl Math 199:424–431
31. Lamba H, Seaman T (2006) Mean-square stability properties of an adaptive time-stepping SDE solver. J Comput Appl Math 194:245–254
32. Chantasiriwan S (2000) Inverse determination of steady-state heat transfer coefficient. Int Comm Heat Mass Transf 27(8): 1155–1164
33. Erdogdu F (2005) Mathematical approaches for use of analytical solutions in experimental determination of heat and mass transfer parameters. J Food Eng 68:233–238
34. Kusiak A, Battaaglia JL, Marchal R (2005) Influence of CrN coating in wood machining from heat flux estimation in the tool. Int J Therm Sci 44:289–301
35. Cohen K, Siegel S, McLaughlin (2006) A heuristic approach to effective sensor placement for modelling o a cylinder wake. Comput Fluids 35:103–120
36. Chen CK, Wu LW, Yang YT (2006) Application of the inverse method to the estimation of heat flux and temperature on the external surface in laminar pipe flow. Appl Therm Eng 26:1714–1724
37. Benjamin SF, Roberts CA (2002) Measuring flow velocity at elevated temperature with a hot wire anemometer calibrated in cold flow. Int J Heat Mass Transf 45:703–706
38. Uselton S, Ahrens J, Bethel W, Treinish L (1998) Multi-source data analysis challenges. In: Proceedings of IEEE Vis 98(VIZ98)
39. Emery AF, Nenarokomov AV, Fadale TD (2000) Uncertainties in parameter estimation: the optimal experiment design. Int J Heat Mass Transf 43:3331–3339
40. Refsgaard JC, Henriksen HJ (2004) Modelling guidelines terminology and guiding principles. Adv Water Resour 27:71–82
41. Lauwagie T, Sol H, Heylen W (2006) Handling uncertainties in mixed numerical-experimental techniques for vibration based material identification. J Sound Vib 291:723–739
42. Ramroth WT, Krysl P, Asaro RJ (2006) Sensitivity and uncertainty analysis for FE thermal model of FRP panel exposed to fire. Compos Part A 37:1082–1091
43. Hsu PT (2006) Estimating the boundary condition in a 3D inverse hyperbolic heat conduction problem. Appl Math Comput 177:453–464